EPJ Web of Conferences **275**, 01007 (2023) https://doi.org/10.1051/epjconf/202327501007
11th European Summer School on Experimental Nuclear Astrophysics

Influence of crystal structures on electron screening

Aleksandra Cvetinović[1,⋆], *Dijana* Djeordjić[2,3], *Giovani Luca* Guardo[4,5], *Mitja* Kelemen[1,2], *Marco* La Cognata[4], *Livio* Lamia[4,5,6], *Sabina* Markelj[1], *Rosario Gianluca* Pizzone[4], *Thomas* Schwarz-Selinger[7], *Isabela* Tišma[8], *Matjaž* Vencelj[1], *Jelena* Vesić[1], and *Matej* Lipoglavšek[1]

[1] *Jožef Stefan Institute, Ljubljana, Slovenia*
[2] *Jožef Stefan International Postgraduate School, Ljubljana, Slovenia*
[3] *University of Banja Luka, Faculty of Mechanical Engineering, Banja Luka, Bosnia and Herzegovina*
[4] *INFN-Laboratori Nazionali del Sud, Catania, Italy*
[5] *Dipartimento di Fisica e Astronomia "E. Majorana", University of Catania, Catania, Italy*
[6] *Centro di Fisica Nucleare e Struttura della Materia, University of Catania, Catania, Italy*
[7] *Max Planck Institute for Plasma Physics, Garching, Germany*
[8] *Rudjer Bošković Institute, Zagreb, Croatia*

Abstract. For nucleosynthesis calculations, precise reaction rates should be known at energies within the Gamow window. At these energies, electron screening cannot be neglected. Despite the significance of the effect, a huge disagreement between experimental data and theoretical predictions is still not understood. In order to address to this problem, we investigated the dependence of the electron screening potential on the target host lattice structure by measuring the rate of the ^{2}H(^{19}F,p)^{20}F reaction in zirconium, titanium and palladium targets containing deuterium .

1 Introduction

Accurate measurements of nuclear reactions between charged particles show an unexpectedly large enhancement of the cross section at energies within the Gamow window [1]. The enhancement is attributed to the presence of atomic electrons that screen the nuclear charge, effectively reducing the repulsive Coulomb barrier between interacting particles. Consequentially, the probability for the nuclear reaction is increased. The screening effect dominates reaction rates at thermonuclear energies, but at higher energies its contribution can be neglected. Moreover, experimental results (see Refs. [2–9] and references therein) unequivocally indicate the incorrectness of available models, since the amplitudes of measured screening potentials (U_e) strongly exceed the theoretically predicted values [10]. While the theory predicts an electron screening potential independent of the target host material, measurements report a strong dependence of the cross section enhancement on the target host and the metallurgy of the solid lattice [9]. Namely, when gaseous targets are used, the electron screening potentials remain within the adiabatic limit. However, the cross sections are especially enhanced in cases when the target nuclei are implanted into a solid lattice, often more than an order of magnitude above the predictions. Therefore, the problem remains and has to be solved, before one can apply electron

⋆e-mail: aleksandra.cvetinovic@ijs.si

© The Authors, published by EDP Sciences. This is an open access article distributed under the terms of the Creative Commons Attribution License 4.0 (http://creativecommons.org/licenses/by/4.0/).

screening to the nucleosynthesis calculations and try to understand what would be the consequences of electron screening in the thermonuclear processes in stellar plasma.

A simplified static theoretical approach [10] is usually employed for electron screening calculations, which assumes that the atomic electrons form a uniformly charged spherical shell, with an atomic radius R_a, around target nuclei. The reaction cross section $\sigma(E)$ is then enlarged by an enhancement factor f defined as the ratio of the screened and bare-nucleus cross sections:

$$f = \frac{\sigma(E + U_e)}{\sigma(E)}, \tag{1}$$

where E represents the energy in the center of mass system and U_e the electron screening potential that can be simply calculated as:

$$U_e = \frac{Z_1 Z_2 e^2}{4\pi\epsilon_0 R_a}, \tag{2}$$

where Z_1 and Z_2 are the charge numbers of the projectile and target nuclei. This result is called the adiabatic limit [10] and represents the maximum value for the screening potential. To simplify the analysis, when nuclear reactions are studied at low energies, the cross section σ is usually defined using the astrophysical $S(E)$-factor, which in the case of non-resonant reactions varies smoothly with energy [1]:

$$\sigma(E) = \frac{S(E)}{E} e^{-2\pi\eta}. \tag{3}$$

Here η is the Sommerfeld parameter.

2 Experiment

The experimental study of the electron screening effect was performed using the 2 MV Tandetron accelerator at the Microanalytical Center of Jožef Stefan Institute (JSI). We investigated the dependence of the electron screening potential on the target host lattice structure by measuring the rate of the ^{2}H(^{19}F,p)^{20}F reaction in thick zirconium, two thick and one thin titanium and two different thick palladium deuterium-containing targets. Based on our previous findings [9] suggesting that the preparation of the host material and location of the target nuclei in the metallic lattice can influence the electron screening, our goal was to find different values of U_e in at least two targets and then to understand which parameters of those targets differ and cause high electron screening. Our latest results are presented below.

2.1 Target preparation

For our study of electron screening, we chose Zr, Ti and Pd as hosting materials because these metals have the ability to absorb large volumetric quantities of deuterium. The Zr target was a 0.25 mm thick 99.8 % pure foil purchased at ChemPUR. The first Ti target was a 1 mm thick 99 % pure foil purchased at Goodfellow. The second titanium target was made by pressing the TiD powder to a thickness of 1 mm into a cylindrical hole (14 mm diameter and 1 mm depth) in 2 mm thick Cu backing. The third Ti target was a 330 nm thick Ti evaporated on Ta backing. The first Pd target was 100 μm thick soft Pd foil purchased at ChemPUR and the second one was a 100 μm thick hard Pd foil produced according to our specifications at Zlatarna Celje. It was cold rolled from a thickness of about 2.5 mm to 0.1 mm. This foil was much less flexible than Chempur's one. Purities of both foils were above 99.9%. In

order to prepare the targets for electron screening studies, Zr and Ti foils were implanted using Tectra IonEtch ion gun. The foils have been bombarded for about 24 h with the deuterium beam accelerated by an extraction voltage of 3.5 kV. The beam current was 400 μA. During implantation, the targets were mounted on a massive copper holder which effectively prevented substantial heating of the foils. Due to the deuterium diffusion, foils had high deuterium concentrations at depths much higher than the implantation depth at 3.5 keV (41 nm [11]). Pd foils were loaded by leaving the palladium in deuterium gas at the pressure of 1 bar and temperature of 24°C for 24 hours. In the soft Pd foil, maximum concentrations of 70% of D per metallic atom were achieved. This is consistent with the limit of hydrogen absorption at normal pressures [12]. However, the hard Pd foil could be loaded only up to 47% of D per metallic atom.

The deuterium depth distribution in the targets was determined with the Nuclear Reaction Analysis (NRA) technique [13]. For this purpose, high energy protons emitted in the ^{2}H(^{3}He,p)^{4}He reaction were measured at six ^{3}He energies, in an energy region from 0.629 to 4.297 MeV. The deuterium depth profiles were obtained by fitting the NRA spectra using the SIMNRA code [14]. Fig. 1 shows deuterium depth distributions measured in our targets after the ^{19}F+d experiment. Deuterium concentration errors are estimated to be ~4%. Note that the 9.2 MeV ^{19}F ion beam is fully stopped in Pd at the depth of 2.62 μm, in Zr at the depth of 3.91 μm and in Ti at the depth of 4.07 μm.

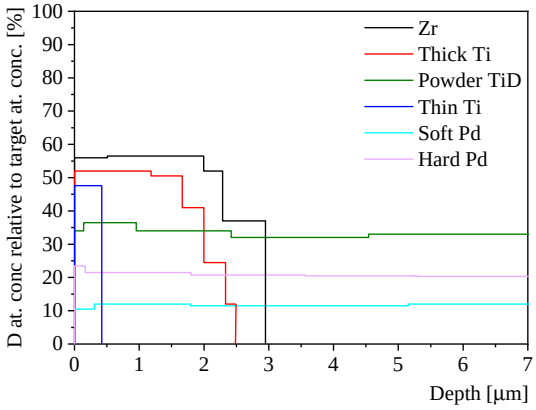

Figure 1. Deuterium concentration relative to the number of target atoms as a function of depth in the target, measured in Zr (black line), thick Ti (red line), powder Ti (green line), thin Ti (blue line), soft Pd (purple line) and hard Pd (light blue line) targets using the Nuclear Reaction Analysis technique. Deuterium concentration errors are estimated to be ~4%.

2.2 Experimental setup

The reaction between ^{2}H and ^{19}F produces the radioactive ^{20}F which decays with a half-life of 11 s through β- decay to the stable ^{20}Ne. ^{20}Ne de-excites to the ground state by emitting a γ-ray with an energy of 1634 keV. The branching ratio for this transition is 99.9% [15]. To determine the screened cross section, yield of these gammas was measured using a High-Purity Germanium (HPGe) detector positioned 57 mm from the target at an angle of 135° with respect to the ^{19}F ion beam direction. The intrinsic detector efficiency was 53% relative to a 3" x 3" NaI detector. It had an efficiency of 0.6% and a resolution of 2.2 keV at the 1.3 MeV ^{60}Co peak. The ^{19}F ion beam with currents of about 0.5 μA was used to study the ^{19}F+d reaction in an energy range between 3.089 and 9.200 MeV. The numbers of incident ions were deduced by measuring the charge collected on the electrically isolated target chamber.

In order to effectively prevent substantial heating of the targets during the experiment, foils were mounted on a massive copper holder. Targets were positioned in a high vacuum chamber with its surface orientated perpendicularly to the beam direction. During the experiment, we monitored deuterium loss in all targets by repeatedly measuring yields at the beam energy of 7.671 MeV before

and after each measurement at other energies. Almost negligible changes in deuterium concentration were detected in Zr and Ti targets. However, Pd targets showed a loss of deuterium during all measurements. In order to correct for the deuterium loss, we normalized the detected yields for a given beam energy to the average of the two control measurements.

3 Results

In the case of the thin Ti target, the reaction cross section σ was calculated from [16]:

$$N_\gamma = \sigma \epsilon W_\gamma N_F n_D \frac{\rho N_A x}{M}. \tag{4}$$

Here ϵ is the efficiency of the detector, W_γ is the angular distribution factor for emitted γ-rays (W_γ=1 since the γ-ray angular distribution is isotropic after β decay [15]), N_F is the number of incident ^{19}F ions, N_γ is the experimentally measured number of γ rays and the value $n_D \frac{\rho N_A d}{M}$ represents the surface density of deuterium atoms in the target (here n_D is the number of deuterium atoms per crystal lattice atom, x is the target thickness, N_A, ρ and M are the Avogadro's number, target density and molar mass).

In the case of thick targets, Eq. 4 has to be transformed into a differential form and integrated over energies from the beam energy E_0 to E_x:

$$N_\gamma = N_F n_D \frac{\rho N_A}{M} \int_{E_0}^{E_x} \epsilon W_\gamma \frac{\sigma_E}{dE_F/dx} dE_F, \tag{5}$$

where E_x is the remaining energy of the beam after passing trough the target layer implanted with D. The stopping power dE_F/dx was calculated using the SRIM code [11].

Since there is no available cross section for the ^{19}F+d reaction in the studied energy region, to determine the bare-nucleus cross section, we measured the same reaction, but this time in forward kinematics, in which we never observed a large electron screening effect, except for the p+d reaction [17, 18]. The measurement was performed with the 3MV accelerator at Max Planck Institute for Plasma Physics in Garching in an energy range from E_d=(303 to 998 keV) on thin CaF_2 targets positioned perpendicularly to the beam. The 1634 keV γ-ray yield was measured using the same HPGe detector as was used for the experiments in inverse kinematics, but this time positioned at an angle of 0° with respect to the ion beam direction, 4.82 mm from the target. More details on the used experimental technique and the cross section data are in [19]. In this experiment, by fitting the experimental data we obtained the bare-nucleus astrophysical S-factor (center-of-mass energy E is given in MeV.):

$$S(E)_{^{19}F+d} = 19380 - 4596E - 3218E^2\,[MeVb]\,, \tag{6}$$

that was used to calculate enhancement factors and electron screening potentials for the ^{2}H(^{19}F,p)^{20}F reaction in all our targets. In the upper panel of Fig. 2 we show the integrated enhancement factors as a function of fluorine beam energy in the center-of-mass system that we obtained in three Ti Targets, while integrated enhancement factors obtained in Zr and two Pd targets are shown in the lower panel. The obtained screening potentials for each target are listed in Table 1.

4 Conclusions

We studied the electron screening effect in the ^{2}H(^{19}F,p)^{20}F nuclear reaction on Zr, three different Ti and two different Pd targets containing deuterium. In all targets we measured different values of the

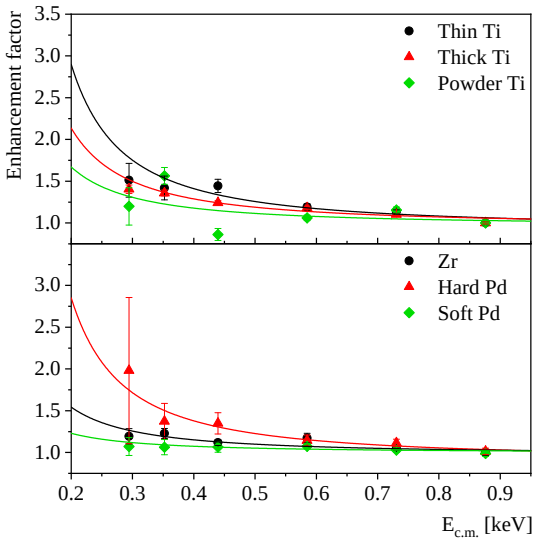

Figure 2. Integrated enhancement factors as a function of the fluorine beam energy in the center-of-mass system for the ^{2}H(^{19}F,p)^{20}F reaction obtained in three Ti targets (upper panel), and in the Zr and two Pd targets (lower panel). Points represent experimental data and the solid lines represent least-squares fits to the data.

Table 1. The electron screening potentials U_e measured in the ^{2}H(^{19}F,p)^{20}F reaction in six different targets in comparison with the predicted screening potential given by the adiabatic model.

Target	U_e [keV]
Zr	7.0±1.9
Soft Pd	3.2±1.9
Hard Pd	18.2±3.3
Thin Ti	18.0±4.9
Thick Ti	12.3±2.8
Powder Ti	8.4±9.2
U_{ad} [keV]	2.19

electron screening potentials. In our powder Ti target we did not detect electron screening different from zero, within the error bars (U_e=8.4±9.2 keV). In the soft Pd target the measured screening potential U_e=3.2±1.9 was in agreement with the theoretical value (U_{ad}=2.19 keV). In the remaining four targets we measured high electron screening potentials, that were up to an order of magnitude above the theoretical model. Namely, in Zr target we measured electron screening potential to be U_e=7.0±1.9, in the thick Ti foil U_e=12.3±2.8 and in the thin Ti and Hard Pd targets we measured the highest screening of U_e=18.0±4.9 and U_e=18.2±3.3, respectively. Since in each target we measured a different screening potential for the same nuclear reaction, which is contrary to the predictions given by the available theoretical model, we found that the screening effect is not linked to the static electron densities around interacting nuclei and that probably, a dynamic approach should be applied. Our findings clearly show that electron screening is strongly linked to the host's crystal lattice structure and electron densities at locations of the target nuclei in the metallic lattice. However, in order to understand this link, additional investigations are required. Our future plans are to apply quantitative methods, such as neutron and X-ray diffraction and nuclear magnetic resonance analysis, in order to test this link.

References

[1] C. Iliadis, *Nuclear Physics of Stars - Second, Revised and Enlarged Edition* (Wiley-VCH, Weinheim, 2015)
[2] K. Czerski et al., Europhys. Lett. **68**, 363 (2004)
[3] J. Kasagi et al., J. Phys. Soc. Jpn. **73**, 608 (2004)
[4] F. Raiola et al., J. Phys., G **31**, 1141 (2005)
[5] J. Cruz et al., Phys. Lett., B **624**, 181 (2005)
[6] T. S. Wang et al., J. Phys. G: Nucl. Part. Phys. **34**, 2255 (2007)
[7] A. Huke et al., Phys. Rev. C **78**, 015803 (2008)
[8] M. Lipoglavšek et al., Eur. Phys. J., A **44**, 71 (2010)
[9] A. Cvetinović et al., Phys. Rev., C **92**, 065801 (2015)
[10] H. J. Assenbaum et al., Z. Phys. A: At. Nucl. **327**, 461 (1987)
[11] J. F. Ziegler et al., *The Stopping and Range of Ions in Matter* (Lulu Press Co., Morrisville, NC, 2008) www.srim.org
[12] G. Alefeld and J. Völkl, *Hydrogen in metals II, Application-oriented properties* (1978) 81
[13] P. Petersson, et al., Nucl. Instrum. Methods Phys., B 268, 1838 (2010)
[14] M. Mayer, *SIMNRA User's Guide* (Report IPP 9/113, Max-Planck-Institut für Plasmaphysik, Garching, Germany, 1997) https://mam.home.ipp.mpg.de
[15] D. R. Tilley et al., Nucl. Phys. A **636**, 249 (1998)
[16] C. Rolfs and R. W. Kavanagh, Nucl. Phys. A **455**, 179 (1986)
[17] M. Lipoglavšek et al., Phys. Lett., B **773**, 553 (2017)
[18] J. Vesić et al., Eur. Phys. J., A **50**, 153 (2014)
[19] A. Cvetinović et al., submitted to Phys. Lett., B.